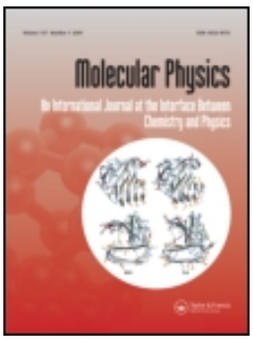

Molecular Physics

ISSN: 0026-8976 (Print) 1362-3028 (Online) Journal homepage: https://www.tandfonline.com/loi/tmph20

Simulation of site-site soft-core liquid crystal models

Gaia Valeria Paolini , Giovanni Ciccotti & Mauro Ferrario

To cite this article: Gaia Valeria Paolini , Giovanni Ciccotti & Mauro Ferrario (1993) Simulation of site-site soft-core liquid crystal models, Molecular Physics, 80:2, 297-312, DOI: 10.1080/00268979300102271

To link to this article: https://doi.org/10.1080/00268979300102271

Published online: 26 Oct 2007.

MOLECULAR PHYSICS, 1993, VOL. 80, NO. 2, 297–312

Simulation of site–site soft-core liquid crystal models

By GAIA VALERIA PAOLINI†
IBM European Center for Scientific and Engineering Computing,
Viale Oceano Pacifico 171, I-00144 Roma, Italy

GIOVANNI CICCOTTI‡
Centre Européen de Calcul Atomique et Moléculaire, Batiment 506,
Université Paris Sud, F-91405 Orsay, France

and MAURO FERRARIO
Dipartimento di Fisica, Sezione di Fisica Teorica, Università di Messina,
Casella Postale 50, I-98166 Sant'Agata di Messina (ME), Italy

(*Received 1 October 1992; accepted 4 January 1993*)

Suggested mechanisms responsible for liquid-crystalline ordering include non-spherical excluded volume effects, anisotropic attraction forces and flexibility. It has been shown using hard-core models that non-spherical excluded volume effects are the essential factor and can qualitatively explain the phenomenology of the problem. However, the simulation of hard-core models is technically demanding. A simpler and more direct alternative is to use a model with a soft-core site–site potential. We employ here a system of molecules composed of a few (11) atoms, constrained to form a multilinear molecule, and in mutual interaction via a continuous repulsive site–site potential of the form r^{-12}. Our results show that such a model is capable of exhibiting nematic and smectic liquid-crystal phases.

1. Introduction

Thermotropic liquid crystals [1, 2] are single-component substances which can order in liquid-crystalline mesophases within certain temperature ranges. Over the last decade, computer simulation has provided insight into the phase behaviour of such systems. Orientational properties have been studied by employing lattice models [3] of particles fixed on lattice sites and interacting through a pair potential depending on their orientation. Computer simulations of anisotropic systems free to translate as well as to rotate are on the other hand complex and very time consuming. Full molecular dynamics simulations of mesogenic systems have been performed following different approaches.

Single-site potentials such as the Gay–Berne molecular potential [4] (derived as a modification of the Berne–Pechukas [5] Gaussian-overlap potential) have been investigated, showing nematic and smectic mesophases [6–10]. The Gay–Berne potential is an interaction applied to the centres of mass of the molecules, with

† Present address: Laboratoire des Solides Irradiés, Ecole Polytechnique, 91128 Palaiseau Cedex, France.

‡ Permanent address: Dipartimento di Fisica, Università 'La Sapienza', Piazzale Aldo Moro 2, I-00185 Roma, Italy.

parameters depending on the mutual orientation of the molecular axes as well as on their separation and is essentially Lennard-Jones in character. It therefore possesses both short-range repulsion and long-range attraction. Its main drawback lies in the fact that it is not transferable, i.e. it cannot be used to construct the interactions of the molecule viewed as an assembly of atoms.

Realistic simulations of mesogenic compounds have been attempted in the last few years by classical molecular dynamics [11–13]. Studies of that kind, however, are somewhat limited by the length of the runs and the size of the system and therefore are not intended to provide a thorough account of the phase behaviour of such compounds. Recently, Wilson and Allen [14] carried out a molecular dynamics simulation of a realistic mesogenic molecule at constant pressure, and over a range of temperatures, generating longer trajectories and showing good agreement with experimental data.

On the other hand, model systems consisting of hard-core anisotropic molecules such as ellipsoids of revolution or spherocylinders have been extensively studied [15–21] showing that steric repulsion is sufficient to describe the occurrence of a number of liquid-crystalline phases. However, the simulation of hard-core models is technically rather complicated.

In the present work we choose a simpler approach: our model consists of a set of linear molecules interacting via a soft-core continuous potential. This approach is more straightforward and less specialized than hard-core or molecular models, and appears as a good candidate for exhibiting liquid-crystalline behaviour, because the potential naturally gives rise to anisotropic excluded volume effects. Indeed, a purely mechanical analysis of the system, based on long molecular dynamics runs over a wide range of temperatures, shows evidence of a rich phase diagram including solid, smectic, nematic and isotropic phases. The thermodynamical analysis of the relative stability of these phases will be the subject of a subsequent study. We stress that, even though the model is conceptually simple, it shares with other polyatomic models the requirement of large computational effort to generate stable trajectories while avoiding small-system size effects.

The paper is organized as follows. In section 2 we describe the model used and the details of the simulations. Some quantities of interest for the characterization of the phase behaviour are described in section 3, while section 4 contains our results. Concluding remarks are given in section 5.

2. Model and implementation

The model employed is a system of N rigid linear molecules ($N = 600$ in all calculations reported here, previous studies with smaller N were hampered by small-size effects) with periodic boundary conditions in the three directions. Each molecule is composed of 11 centres of force and interacts with other molecules via a site–site atomic potential of the form

$$V(r) = 4\epsilon(\sigma/r)^{12},$$

where $r = |\mathbf{r}_i - \mathbf{r}_j|$ is the distance between two atoms belonging to different molecules. The potential parameters are $\sigma = 3{\cdot}9$ Å and $\epsilon = 6{\cdot}0 \times 10^{-22}$ J. Of the 11 sites of each molecule, only the two at the extremes are true atoms, each of mass $m = 1{\cdot}993 \times 10^{-23}$ g, while the others are massless centres of force [22], i.e. they contribute to the site–site interactions but bear no mass. The centres of force are

constrained [22] on a line, at an interatomic distance $\sigma^*/2$, where $\sigma^* = 1{\cdot}2\sigma$ is chosen as the effective atomic diameter. A cut-off $r_C = 1{\cdot}7\sigma$ is used for pair interactions. Such a model is geometrically comparable to a spherocylinder of length-to-width ratio $L/D \approx 5$. We chose this ratio on the basis of [20] (in which a system of hard spherocylinders for various length-to-width ratios is studied) in order to be able to simulate a system with a phase diagram spanning various mesophases.

We simulated a system in conditions of fixed temperature and pressure by implementing the Nosé [23] canonical ensemble technique coupled with the Parrinello–Rahman [24, 25] method, allowing the shape as well as the volume of the computational box to fluctuate for the whole set of temperatures studied. In this way we attempted to avoid any possible metastability imposed by the constraint of constant-cell simulations.

At a fixed pressure $P = 4\,\text{kbar}$ we raised the temperature T, in steps $\Delta T = 100\,\text{K}$ (occasionally $\Delta T = 50\,\text{K}$), starting from a solid configuration at $T = 50\,\text{K}$ and allowing the system to equilibrate for about 100 ps at each temperature. We explored the temperature range from 50 to 1800 K. As an initial solid configuration we used the hexagonal close packed (hcp) one, stretched along the x-axis, with all the molecules initially parallel to this direction. This structure is defined as two interpenetrating simple hexagonal lattices, displaced from one another by $\mathbf{a}/2 + \mathbf{b}/3 + \mathbf{c}/3$, where $\mathbf{a}, \mathbf{b}, \mathbf{c}$ are the cell vectors. We chose such an initial condition because of its good close-packing properties. The hcp lattice is AB-stacked along the direction of stretching x and it is quite close to the ABC-stacked structure generating the fcc stretched lattice studied by Veerman and Frenkel [21]. The initial volume of the computational box is $V = 0{\cdot}309 \times 10^6\,\text{Å}^3$, corresponding to a number density $\rho = 0{\cdot}00194\,\text{Å}^{-3}$. If we normalize this number by using the total excluded volume v_{ex} of a spherocylinder with the equivalent length-to-width ratio, we obtain a reduced density $\rho^* = \rho v_{ex} = \rho[(17/12)\pi\sigma^{*3}] = 0{\cdot}9$.

As pointed out by Nosé and Klein [26], in molecular systems, using the Parrinello–Rahman technique, the computational box can undergo overall rotations which have no physical meaning. To avoid such a problem, one possible solution is to fix the absolute orientation of the box in the reference system [27]. In this case we can choose **a** oriented along x, and **b** to span the xy-plane, being left with only six variables to describe the box. At $t = 0$, in particular, we have: $\mathbf{a} = (a_x, 0, 0)$, $\mathbf{b} = (0, b_y, 0)$ and $\mathbf{c} = (0, c_y, c_z)$. The resulting computational box is monoclinic, with angles $\alpha = \beta = 90°$, $\gamma = 60°$. Equilibration of the initial configuration at $T = 50\,\text{K}$ and $P = 4\,\text{kbar}$ shows that this structure is stable. We did not, however, investigate the existence and stability of other possible solid structures, because this would go beyond the scope of this work, the aim of which is the characterization of liquid-crystalline mesophases in our model system.

The equations of motion were integrated using the Verlet central difference algorithm, adapted to the method of constraints in cartesian coordinates and to the Parrinello–Rahman technique [22]. The time step is $\Delta t = 5\,\text{fs}$ for temperatures up to $T = 1000\,\text{K}$, 2 fs for temperatures between $T = 1000$ and 1400 K and 1 fs at higher temperatures, to properly treat the fast librational motions in the system.

3. Order parameters

From a microscopic point of view, the various mesophases can be described in terms of the properties of molecular distribution functions. For $i = 1 : N$, let $\mathbf{R}_i$ be

the centre-of-mass positions and $\mathbf{\Omega}_i$ the orientations of the molecules with respect to a frame fixed in the laboratory coordinate system. We can to a good approximation identify the nematic director $\hat{\mathbf{n}}$ (of which we give an operative definition in section 3.1) with one of the coordinate axes. $\mathbf{\Omega}$ denotes Euler angles (θ, ϕ, ψ) for a general molecule, while for a linear molecule orientations can be described with polar angles and we have $\mathbf{\Omega} = (\theta, \phi)$. We define the single-particle distribution function as

$$\mathscr{P}^{(1)}(\mathbf{R}_1, \mathbf{\Omega}_1) = \frac{N}{Q_N} \int \mathrm{d}\mathbf{R}^{N-1}\, \mathrm{d}\mathbf{\Omega}^{N-1}\, \mathrm{d}\mathbf{P}_R^N\, \mathrm{d}\mathbf{P}_\Omega^N\, \mathrm{e}^{-\beta H}, \tag{1}$$

where H is the Hamiltonian of the system, $\beta = 1/kT$, Q_N is the canonical partition function for N molecules, and $\mathbf{P}_R$ and $\mathbf{P}_\Omega$ are the conjugate momenta to $\mathbf{R}$ and $\mathbf{\Omega}$. The integration extends to the N momenta and to molecules from 2 to N for the configurational part. Expansion coefficients of $\mathscr{P}^{(1)}(\mathbf{R}_1, \mathbf{\Omega}_1)$ in a suitable basis set allow the definition of some order parameters.

In a *nematic* phase, positional order is absent and we can write equation (1) as

$$\mathscr{P}^{(1)}(\mathbf{R}, \mathbf{\Omega}) = \rho \tilde{f}(\mathbf{\Omega}),$$

where ρ is the number density of molecules and $\tilde{f}(\mathbf{\Omega})$ is the orientational distribution function, normalized as

$$\int \mathrm{d}\mathbf{\Omega}\, \tilde{f}(\mathbf{\Omega}) = \int_{-1}^{1} \mathrm{d}\cos\theta \int_0^{2\pi} \mathrm{d}\phi \int_0^{2\pi} \mathrm{d}\psi\, \tilde{f}(\theta, \phi, \psi) = 1.$$

This can be expanded in terms of the Wigner rotation matrices, or generalized spherical harmonics [3] D_{mn}^L

$$\tilde{f}(\mathbf{\Omega}) = \sum_{Lmn} f_{Lmn} D_{mn}^L(\mathbf{\Omega}),$$

with

$$f_{Lmn} = \frac{2L+1}{8\pi^2} \langle D_{mn}^{L*} \rangle,$$

where the factor $(2L+1)/8\pi^2$ comes from the orthogonality relations of the D_{mn}^L. The brackets denote an average over the orientations $\mathbf{\Omega}$ weighted with $\tilde{f}(\mathbf{\Omega})$. The $\langle D_{mn}^{L*} \rangle$ completely define $\tilde{f}(\mathbf{\Omega})$ and play the role of orientational order parameters. Their number can be largely reduced by using the symmetries of the system. Linear molecules are cylindrically symmetric and thus the orientational distribution is independent of ψ $(n = 0)$. Optically uniaxial phases possess one symmetry axis—the nematic director $\hat{\mathbf{n}}$—therefore there is invariance under rotation around $\hat{\mathbf{n}}$ and the distribution is also independent of ϕ $(m = 0)$. The D_{00}^L then reduce to the Legendre polynomials $P_L(\cos\theta)$. If, additionally, the phase has a symmetry plane perpendicular to the director, only even powers of L are to be considered, and we have:

$$\tilde{f}(\mathbf{\Omega}) = \frac{f(\theta)}{4\pi^2} = \sum_{L=0}^{\infty} \left[\frac{4L+1}{8\pi^2} \langle P_{2L}(\cos\theta) \rangle \right] P_{2L}(\cos\theta),$$

where $\int_{-1}^{1} f(\theta)\, \mathrm{d}\cos\theta = 1$ and $\langle P_{2L}(\cos\theta) \rangle$ are the orientational order parameters. The lowest non-trivial order parameter, $\langle P_2 \rangle = \frac{1}{2}\langle 3\cos^2\theta - 1 \rangle$ is usually referred to as the nematic order parameter. Experimentally, both $\langle P_2 \rangle$ and $\langle P_4 \rangle$ can be determined by Raman scattering [1].

In a *smectic* phase, the distribution functions depend on position as well as orientation. For positional order in one dimension (e.g. x) the singlet distribution function depends not only on the angles Ω but also on the one-dimensional coordinate. It can therefore be expanded in Fourier series for positions and in Wigner series for orientation, and will be described by positional and orientational order parameters a_{LM}. For a linear molecule and a uniaxial phase we can write [3]

$$P^{(1)}(x,\theta) = \sum_{LM} a_{LM} \exp(2\pi i M x/d)\, P_L(\cos\theta),$$

where d is the average interlayer spacing, $P^{(1)}(x,\theta)$ is normalized as

$$\int_{-1}^{1} \mathrm{d}\cos\theta \int_{d} \mathrm{d}x\, P^{(1)}(x,\theta) = N,$$

and

$$a_{LM} = \frac{(2L+1)}{2d} \langle \exp(2\pi i M x/d)\, P_L(\cos\theta)\rangle, \tag{2}$$

are the orientational–positional order parameters. Purely positional order can then be described by setting $L = 0$ in equation (2), thus getting

$$a_{0M} = \frac{1}{2d} \langle \exp(2\pi i M x/d)\rangle \tag{3}$$

3.1. *Collective orientational order parameters*

In a computer simulation, the orientation of the nematic director is not known *a priori* and will generally fluctuate during the time evolution of the system. We choose the nematic director $\hat{\mathbf{n}}$ as the unit vector that maximizes the expression [3]

$$\begin{aligned}\epsilon(\hat{\mathbf{n}}') &= \frac{1}{N}\sum_{i=1}^{N}[\tfrac{3}{2}(\hat{\mathbf{n}}'\cdot\hat{\mathbf{u}}_i)^2 - \tfrac{1}{2}] \\ &= \hat{\mathbf{n}}'\cdot\mathbf{Q}\cdot\hat{\mathbf{n}}',\end{aligned}$$

with respect to $\hat{\mathbf{n}}'$. The maximum $\epsilon(\hat{\mathbf{n}})$ is the instantaneous *orientational order parameter*. Here $\hat{\mathbf{u}}_i$ are the unit vectors describing the orientations of molecular axes in the laboratory frame, and

$$\mathbf{Q} = \frac{1}{N}\sum_{i=1}^{N}(\tfrac{3}{2}\hat{\mathbf{u}}_i\hat{\mathbf{u}}_i - \tfrac{1}{2}\mathbf{I}),$$

is the tensor associated to the order parameter [3, 15]. The instantaneous orientational order parameter is then equal to $\lambda_{\max}$, the maximum eigenvalue of $\mathbf{Q}$, and $\hat{\mathbf{n}} = \hat{\mathbf{n}}'(\lambda_{\max})$ is the corresponding eigenvector. What we do in practice is compute $\mathbf{Q}$ along a trajectory of the system, diagonalize it, and estimate the ensemble average $\langle P_2\rangle$ with the average over time of $\lambda_{\max}$. We call this average $\bar{P}_2^{(a)}$. Thus

$$\bar{P}_2^{(a)} = \lim_{\tau\to\infty}\frac{1}{\tau}\int_0^{\tau}\lambda_{\max}(t)\,\mathrm{d}t. \tag{4}$$

Orientational order between pairs of molecules can be monitored via the Lth rank *orientational correlation functions* [3]

$$G_L(R) = \frac{\langle P_L(\hat{\mathbf{u}}_i\cdot\hat{\mathbf{u}}_j)\delta(R_{ij}-R)\rangle}{\langle\delta(R_{ij}-R)\rangle} \tag{5}$$

where the brackets denote an ensemble average and $R_{ij} = |\mathbf{R}_i - \mathbf{R}_j|$. The $G_L(R)$ expresses the correlation in orientation between two molecules at a given distance R. For small separations $G_L(R)$ defines the short-range order, while for large R it measures the long-range order. In the disordered phase, G_L decays to zero, while in the ordered phase it decays to the square of the orientational order parameter [3]

$$\lim_{R\to\infty} G_L(R) = \langle P_L \rangle^2, \tag{6}$$

thus giving an alternative way to estimate the nematic order parameter from simulation data. Hereafter we will call $\bar{P}_L^{(b)}$ the order parameters computed via equation (6).

3.2. *Collective positional order parameters*

3.2.1. *Bond order parameter*

To monitor the onset of a smectic phase with two-dimensional liquid layers from a solid phase we computed the bond order parameter Ψ_6^2, defined as [19]

$$\Psi_6^2 = \frac{1}{9N^2}\left|\sum_{i>j} e^{6i\theta_{ij}}\right|^2 \tag{7}$$

where θ_{ij} is the angle between the projection of R_{ij} onto the yz-plane and the y-axis, the sum extending to nearest neighbours on the yz-plane (roughly corresponding to the plane of the layers). By construction, $\Psi_6^2 = 1$ for a perfect hexagonal lattice, while $\Psi_6^2 \approx 0$ for a completely disordered fluid. We note that by using this parameter alone we are not able to distinguish between a truly solid phase and a smectic-B phase, with three-dimensional order. Therefore such a phase, if it exists, should be identified in a different way.

3.2.2. *Density along nematic director*

We computed the average density of molecules along the nematic director $\hat{\mathbf{n}}$ via the formula

$$\rho(\xi) = \left\langle \sum_i \delta(\xi_i - \xi) \right\rangle \tag{8}$$

with

$$\xi_i = (\mathbf{R}_i - \mathbf{R}_o)\cdot\hat{\mathbf{n}}$$

where $\mathbf{R}_o$ is the centre of mass of the whole system, $\int \rho(\xi)\,d\xi = N$, and the density is time-averaged over an equilibrium trajectory.

3.2.3. *Pair correlation functions*

Order in the positions of the centres of mass can also be detected by computing the orientationally averaged pair correlation function $g(R)$ [28] of the centres of mass. In principle the pair correlation function does not have a radial dependence and the only meaning of $g(R)$ is that of an isotropic average. However, the range in which the x-dependence appears is disjoint from that in which the (y, z)-structure manifests itself, because in our system the average interlayer spacing is much larger than the distance of neighbour particles in a layer. As a result the $g(R)$ we obtain with our spherical cut-off gives a good representation of the order in the yz-plane, as long as an inter-layer order exists. To inspect layer-by-layer positional order as well, we chose to divide the computational box into six subcells, centred around each

layer, and to compute the pair correlation function restricted to each layer. We denote this by $g(R;l)$, where $l = 1:6$ indicates the layer considered. This way we were able to monitor the onset of liquid-like ordering in a smectic phase, for each layer separately.

3.2.4. *Smectic order parameter*

We estimated the smectic order parameter for $M = 1$ in equation (3) by calculating the translationally invariant quantity [12]

$$\hat{\tau} = 2\bar{d}\,\|a_{01}\| = \left\| \left\langle \frac{1}{N} \sum_j \exp[(2\pi i/\bar{d})\hat{\mathbf{n}} \cdot \mathbf{R}_j] \right\rangle \right\|, \tag{9}$$

where $\hat{\mathbf{n}} \cdot \mathbf{R}_j$ is the projection of the centre-of-mass of molecule j on the nematic director $\hat{\mathbf{n}}$, $\|\cdots\|$ indicates the norm of a complex number, and $\bar{d}$ is the average spacing between layers, drawn *a posteriori* from the simulation data. The average in equation (9) is a time average over an equilibrium trajectory.

3.3. *Diffusion*

In a liquid crystal, diffusion is anisotropic and must be written as a tensor quantity $D_{\alpha\beta}$. For a uniaxial system with director along the x-axis we have $D_{xx} = D_{\parallel} \neq D_{yy} = D_{zz} = D_{\perp}$, with zero off-diagonal elements. $D_{\alpha\alpha}$, with $\alpha = x, y, z$, can be obtained from the formula

$$D_{\alpha\alpha} = \lim_{t \to \infty} \frac{\langle \delta R_\alpha^2(t) \rangle}{2t}. \tag{10}$$

The mean-square displacement is computed as

$$\langle \delta R_\alpha^2(t) \rangle = \frac{1}{N\tau_{\max}} \sum_{i=1}^{N} \sum_{\tau=1}^{\tau_{\max}} [R_{\alpha i}(t+\tau) - R_{\alpha i}(\tau)]^2,$$

where $\tau_{\max}$ denotes the number of time origins over which the average is taken.

4. Results

Figures 1(*a*)–(*f*) show snapshots of the system at various temperatures. We started by equilibrating a *solid* configuration at $T = 50$ K, with the system arranged on six layers, each of which containing 100 molecules initially oriented along the x-axis. We note that, to avoid unphysical diffusion driven by the periodic boundary conditions [21] it is necessary that the system be large enough in all directions. Exploratory simulations performed on a smaller system, having only two layers along the x-axis, showed evidence of a columnar phase (crystalline order within a layer, but strong diffusion parallel to the nematic director) which disappeared as the system size was increased.

Throughout the equilibration at $T = 50$ K, the nematic director $\hat{\mathbf{n}}$ remained parallel to the x-direction. The average values of the box-angles $\bar{\alpha} = \bar{\beta} = 90{\cdot}0°$ and $\bar{\gamma} = 59{\cdot}4°$, the value of the bond order parameter $\Psi_6^2 = 0{\cdot}974$, and inspection of the pair correlation function (figure 2) shows that the structure of the centres of mass is distorted very little from the ideal lattice structure. On the other hand, the orientations of the molecules present a herringbone structure along the nematic

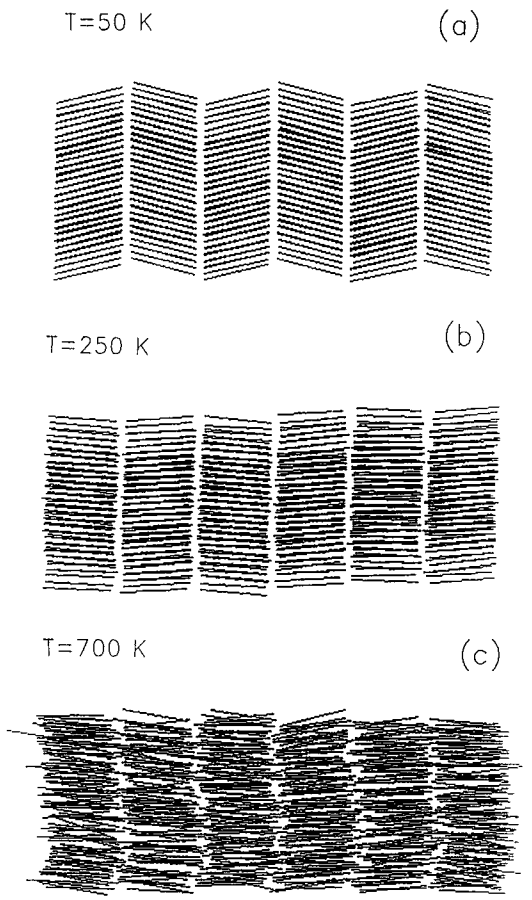

Figure 1. Snapshots of the system at various temperatures. Projection on the xy plane. (*a*) $T = 50\,\mathrm{K}$; (*b*) $T = 250\,\mathrm{K}$; (*c*) $T = 700\,\mathrm{K}$; (*d*) $T = 800\,\mathrm{K}$; (*e*) $T = 700\,\mathrm{K}$, cooled from $T = 800\,\mathrm{K}$; (*f*) $T = 1800\,\mathrm{K}$.

director, visible from the projection of the system on the xy-plane (figure 1(*a*)). The angular distribution function $f(\theta)$ in figure 3 exhibits a peak at $\theta = 14°$. Such structure is not influenced by the volume or shape of the computational box, since these are both allowed to adjust with the Parrinello–Rahman technique, although it is probably favoured by the periodic boundary conditions for an even number of layers. To check for pressure dependence we performed runs at the same temperature ($T = 50\,\mathrm{K}$) and lower pressure $P = 2\,\mathrm{kbar}$ and found that the herringbone structure was greatly reduced, resulting in a tilt angle of 6°.

At $P = 4\,\mathrm{kbar}$, however, as the temperature is increased from $T = 50\,\mathrm{K}$ to $T = 250\,\mathrm{K}$, the molecules tend to reorient along the nematic director and the herringbone structure disappears, as can be seen in figure 1(*b*), while the system still retains translational order in the centres of mass.

Figure 2 shows the orientationally averaged pair correlation function of the centres of mass $g(R)$ for temperatures between $T = 250\,\mathrm{K}$ and $T = 800\,\mathrm{K}$. In this temperature range the system gradually goes from a solid phase to a *smectic* phase (loose layered structure along the nematic director and two-dimensional liquid ordering within a layer) at $T = 700\,\mathrm{K}$.

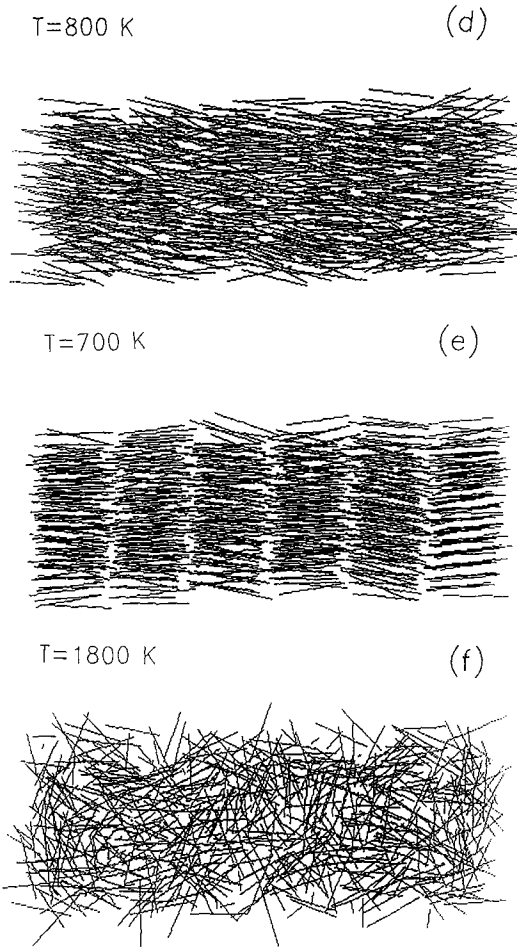

Figure 1 (*continued*).

The intralayer ordering is monitored via the $g(R; l)$ restricted to each layer (figure 4) while the structure along the direction of molecular alignment is checked via the average one-dimensional density $\rho(\xi)$ (figure 5) defined in equation (8).

Inspection of the snapshots of individual layers reveals that the system at $T = 650\,\mathrm{K}$ still has an ordered intralayer structure, although fluctuations are high, as shown by the shape of the $g(R; l)$ in figure 4. A well defined layered structure is present. The mean square displacement parallel and perpendicular to the direction of molecular alignment (figure 6) at $T = 650\,\mathrm{K}$ indicates negligible diffusion at this temperature.

At $T = 700\,\mathrm{K}$ the intralayer structure is lost. At this temperature the pair correlation function assumes a typical liquid-like behaviour, as shown in figure 4. On the other hand, the system still retains a well-defined layered structure as can be seen from the projection on the xy-plane shown in figure 1(*c*) as well as from the structure of $\rho(\xi)$ in figure 5. At this temperature, however, inter-layer diffusion is present. This can be detected visually by taking snapshots of the system and colouring differently molecules initially assigned to different layers. While at $T = 650\,\mathrm{K}$ no molecule has moved from one layer to another, after equilibrating at $T = 700\,\mathrm{K}$ the colours tend

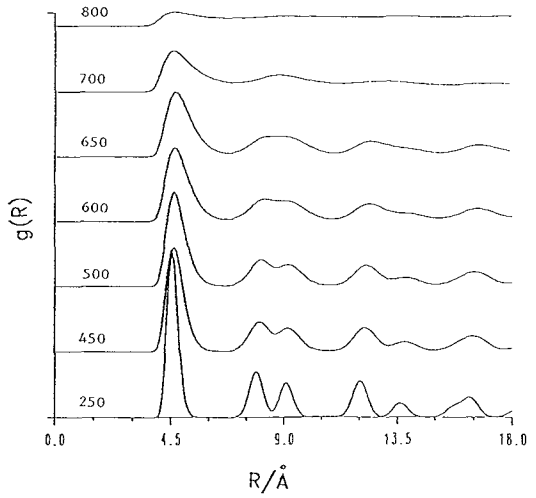

Figure 2. Total pair correlation function of the centres of mass $g(R)$ for temperatures $T = 250$, 450, 500, 600, 650, 700 and 800 K.

to mix up within the same layer. The linear increase of the parallel mean square displacement (figure 6) confirms this behaviour.

The smectic layers are slightly tilted with respect to the nematic director (which is oriented along the x-axis). The tilt direction [1] is uniform within the layers; the average tilt angle [8] is $\phi_{\text{tilt}} \simeq 3$–$4°$ with fluctuations of the order of 50% during 50 ps. Due to the finite size of the sample it is not possible to ascertain whether this is a true smectic-A phase or a tilted smectic-C phase (i.e. a smectic phase in which the nematic director is not orthogonal to the layers). Experimentally, however, only orthogonal smectic phases are observed in non-polar compounds [1], while smectic-C phases are usually associated to the presence of permanent dipole moments.

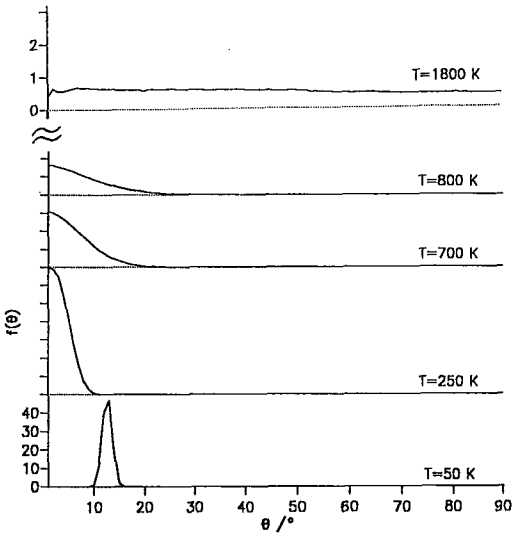

Figure 3. Normalized angular distribution function $f(\theta)$ for temperatures $T = 50$, 250, 700, 800, and 1800 K. Note the change of scale for $T = 1800$ K.

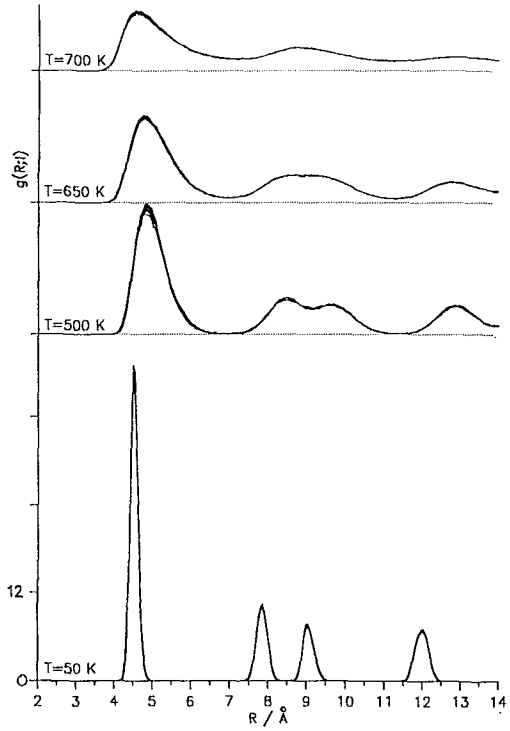

Figure 4. Pair correlation function $g(R;l)$ computed on single layers for temperatures $T = 50$, 500, 650, and 700 K. For each temperature, the $g(R;l)$ for $l = 1 : 6$ are superimposed.

Table 1 reports the values of volume and order parameters defined in section 3 for the temperatures studied. The average interlayer spacing $\bar{d}$ shown in column eight is the value for which the smectic order parameter $\bar{\tau}$ along an equilibrium trajectory was found maximum. The layer thickness is slightly smaller than the length of a molecule ($l \approx 28{\cdot}1$ Å) and linearly increasing with temperature, apart from the values

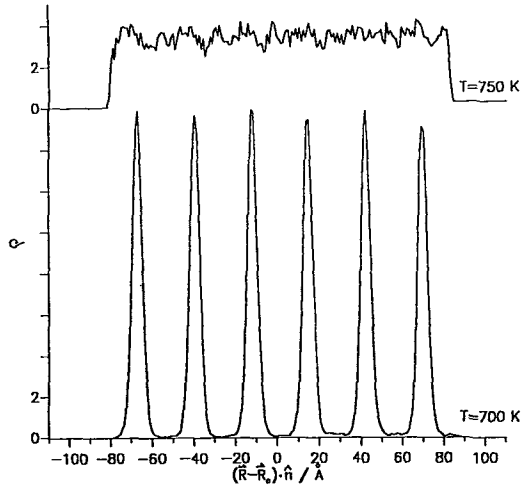

Figure 5. Average number density $\rho(\xi)$ along the nematic director for temperatures $T = 700$ and 750 K.

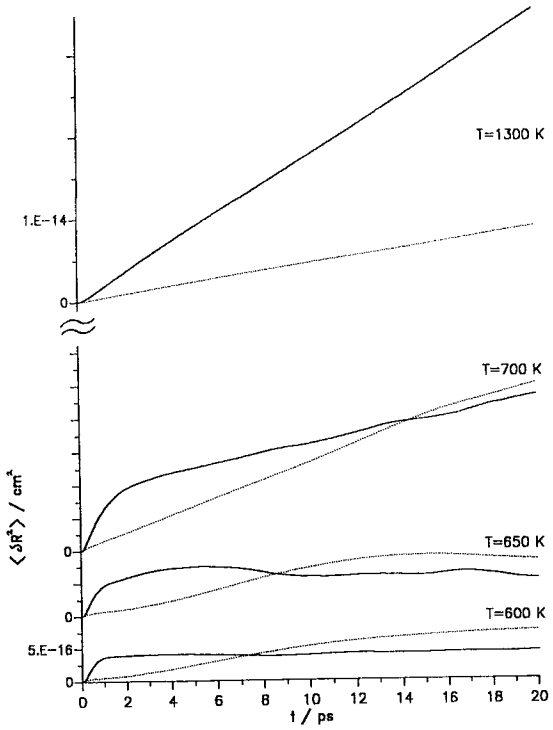

Figure 6. Mean square displacements for temperatures $T = 600$, 650, 700, and 1300 K. Solid line: $\langle \delta R_{\parallel}^2 \rangle$. Dotted line: $\langle \delta R_{\perp}^2 \rangle$. Note the change of scale for $T = 1300$ K.

at $T = 750$–800 K. These values are only indicative, however, because in this temperature range the system has lost its layered structure and $\bar{\tau}$ becomes very small with large fluctuations for all values of $\bar{d}$.

The smectic layers do not possess bond order, as we can see from the values of the bond order parameter Ψ_6^2, which goes from 0·505 at $T = 650$ K (solid) to 0·004 at $T = 700$ K (smectic).

The behaviour of volume $\bar{V}$ and orientational order parameter $\bar{P}_2$ as functions of temperature are shown in figures 7 and 8. From figure 7 we can detect a volume change of about 4% corresponding to the transition from solid to smectic. The smectic region is, however, quite small and is followed by another transition to the nematic phase within about 100 K; besides, the fact that we are spanning the temperature range by fairly large steps ($\Delta T = 50$–100 K) and the purely mechanical analysis performed are not sufficient to draw conclusions on the nature of the transition. In the same temperature range the orientational order parameter $\bar{P}_2$ shown in figure 8 changes only slightly, indicating that orientational order remains high. This can be seen also from the angular distribution function (figure 3) and from the long-range behaviour of the Lth rank orientational correlation functions G_L defined in equations (5) and (6) and shown in figure 9 for $L = 2$. We see that while the system retains short-range order at all temperatures, the decay at large R shows a dramatic difference in the various temperature ranges studied.

Figure 8 compares the two methods used to estimate the nematic order parameter $\langle P_2 \rangle$ from the simulation, namely $\bar{P}_2^{(a)}$, the maximum eigenvalue of the tensor $\mathbf{Q}$

Table 1. Molecular dynamics results. The first column reports the different temperatures; the second column shows the corresponding total volumes; columns three to seven report order parameters defined in section 3. $\bar{P}_2^{(a)}$: maximum eigenvalue of **Q** from equation (4); $\bar{P}_L^{(b)}$: $[\lim_{R\to\infty} G_L(R)]^{1/2}$, $L = 2,4$ from equation (6). Column eight shows the average layer thickness. All runs carried out at $P = 4$ kbar and $N = 600$ molecules.

T/K	$\bar{V}/10^6$ Å^3	$\bar{P}_2^{(a)}$	$\bar{P}_2^{(b)}$	$\bar{P}_4^{(b)}$	$\bar{\tau}$	$\bar{\psi}_6^2$	$\bar{d}$/Å
50	0·279	0·915	0·999	0·999	0·995	0·974	26·7
150	0·285	0·971	0·998	0·996	0·988	0·933	26·8
250	0·290	0·986	0·998	0·992	0·986	0·883	27·1
350	0·296	0·984	0·996	0·988	0·982	0·820	27·2
450	0·302	0·983	0·995	0·982	0·970	0·739	27·3
500	0·306	0·977	0·994	0·978	0·971	0·697	27·4
600	0·313	0·972	0·990	0·968	0·952	0·615	27·6
650	0·318	0·970	0·988	0·960	0·905	0·505	27·8
700	0·332	0·950	0·965	0·890	0·845	0·004	27·6
750	0·347	0·918	0·923	0·771	0·068	0·001	29·8
800	0·352	0·905	0·906	0·725	0·068	0·001	29·3
850	0·356	0·878	0·884	0·681			
900	0·361	0·880	0·884	0·675			
950	0·364	0·868	0·873	0·646			
1000	0·369	0·845	0·847	0·592			
1100	0·376	0·816	0·825	0·553			
1200	0·383	0·782	0·795	0·484			
1300	0·392	0·754	0·748	0·412			
1400	0·400	0·652	0·652	0·293			
1500	0·411	0·529	0·525	0·182			
1600	0·427	0·104	0·108	0·0			
1800	0·441	0·068	0·081	0·0			
700[a]	0·331	0·951	0·966	0·893	0·874	0·007	27·6

[a] Cooled from $T = 800$ K (see text).

(equation (4)) and $\bar{P}_2^{(b)}$, the square root of the large separation limit of the orientational correlation function $G_2(R)$ defined in equation (6). The two methods compare very well, apart from at the lowest temperatures. In this case, the first method provides the nematic director of the whole system and thus evidences the

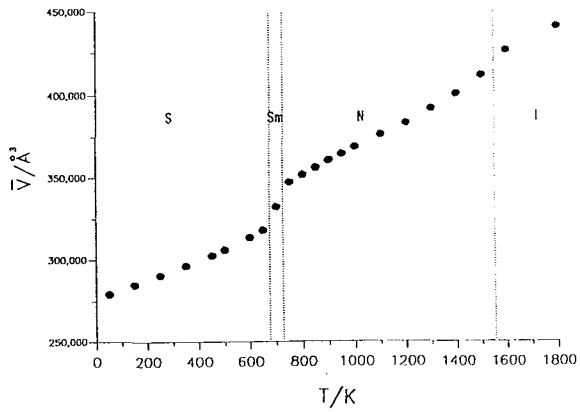

Figure 7. Average volume $\bar{V}$ of the system as a function of temperature. The dotted lines enclose the different phase regions. S: solid; Sm: smectic; N: nematic; I: isotropic phase.

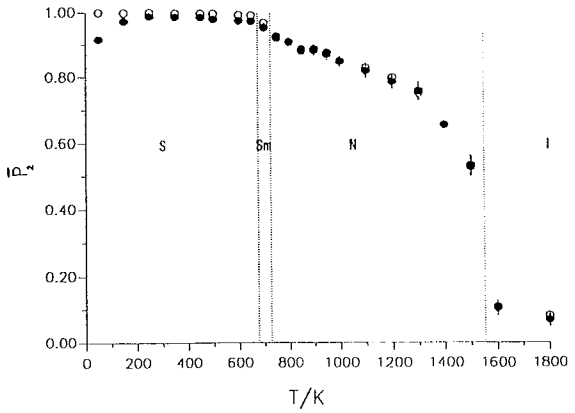

Figure 8. Orientational order parameter $\bar{P}_2$ as a function of temperature. Filled circles: $\bar{P}_2^{(a)}$ from equation (4); open circles: $\bar{P}_2^{(b)}$ from equation (6).

presence of the herringbone structure. The second method, however, because of the spherical cut-off used, is limited to intermolecular distances smaller than the actual layer separation and therefore only takes into account the structure within one layer, which has perfect orientational order, and does not provide the true asymptotic result for large R.

Raising the temperature from $T = 700\,\mathrm{K}$ to $T = 750\,\mathrm{K}$ the layered structure is soon lost—as is apparent comparing the densities in figure 5—and the smectic order parameter $\bar{\tau}$ drops from 0·837 to 0·07 (table 1). Orientational order on the other hand is still high ($\bar{P}_2 = 0{\cdot}9$), thus confirming the onset of a *nematic* phase.

Starting from an equilibrated configuration at $T = 800\,\mathrm{K}$, we slowly cooled it down to $T = 700\,\mathrm{K}$ and found that the system went back to a layered smectic structure very similar to the one previously obtained at the same temperature (figure 1(*e*); table 1). Indeed this is not too surprising, since it should not be too difficult to recover one-dimensional order without getting trapped in a metastable

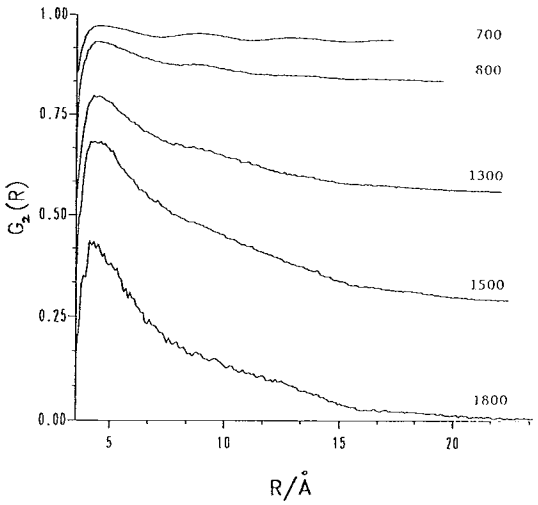

Figure 9. Second rank orientational correlation function $G_2(R)$ for temperatures $T = 700$, 800, 1300, 1500, 1800 K.

state. On the other hand, this confirms the tendency of the system to arrange in a smectic structure within a certain range of temperatures.

The molecules remain orientationally ordered for $T = 800$ to 1500 K. In this temperature interval, the nematic order parameter $\bar{P}_2$ changes continuously from 0·9 to 0·5. The nematic director $\hat{\mathbf{n}}$ is progressively reorienting and forming a non-zero angle with the x-axis, from less than 3° at $T = 700$ K to about 23° at $T = 1500$ K. The angles of the computational box are on the other hand quite stable. Around $T = 700$ K there begins a transition from the angles in the solid phase to values $\bar{\alpha} \approx 87°$, $\bar{\beta} \approx 94°$, and $\bar{\gamma} \approx 70°$, which remain stable over the whole temperature range $T = 800$–1800 K, with fluctuations of order 2%.

At $T = 1600$ K the molecules have almost completely lost their orientational order. The angular distribution function in figure 3 and the snapshot in figure 1(f) confirm that the system at $T = 1800$ K has turned into an *isotropic* fluid. The volume change in the temperature region 1400–1800 K is about 4%, whereas the order parameter (figure 8) drops from $\approx 0{\cdot}5$ to $\approx 0{\cdot}07$. In this range of temperatures the nematic director defined in section 3.1 begins to fluctuate wildly, indicating that there is no stable preferred orientation of the molecules.

We estimated the diffusion coefficients for the various phases from equation (10), finding $D_{\parallel} = 3{\cdot}5 \times 10^{-5}\,\mathrm{cm^2\,s^{-1}}$, $D_{\perp} = 6 \times 10^{-5}\,\mathrm{cm^2\,s^{-1}}$ at $T = 700$ K (smectic phase); $D_{\parallel} = 8{\cdot}5 \times 10^{-4}\,\mathrm{cm^2\,s^{-1}}$, $D_{\perp} = 2{\cdot}2 \times 10^{-4}\,\mathrm{cm^2\,s^{-1}}$ at $T = 1300$ K (nematic phase); $D_{\parallel} \approx D_{\perp} = 4 \times 10^{-4}\,\mathrm{cm^2\,s^{-1}}$, at $T = 1600$ K (isotropic phase). As expected, there is anisotropy in the oriented phases. While $D_{\parallel} < D_{\perp}$ in the smectic phase, because of the layered structure, the situation is reversed in the nematic phase where $D_{\parallel}/D_{\perp} \approx 3{\cdot}9$. This number is much smaller than the value of ≈ 7 which would be derived according to the theoretical estimate given in [29] for hard ellipsoids with the same geometrical anisotropy factor $L/D \approx 5$ and nematic order parameter $\bar{P}_2 = 0{\cdot}75$. These discrepancies, however, might be due to the difference in shape of our molecules with respect to hard ellipsoids. Our value seems in closer agreement with the theory of Chu and Moroi (see [1]) which gives $D_{\parallel}/D_{\perp} \approx 3{\cdot}3$. The quite high numerical values of the diffusion coefficient can be explained by the small mass of the molecules. In fact, by employing reduced units of $(2m/\epsilon\sigma^2)^{1/2}$ we obtain values of $D_{\parallel}$ and $D_{\perp}$ in the range 0·03 to 0·7, in much better agreement with values found by other authors [30].

5. Concluding remarks

We have constructed a model of linear rigid molecules with anisotropy $L/D \approx 5$, interacting via a site–site soft-core potential, showing evidence of the occurrence of different liquid-crystalline mesophases over a wide range of temperatures at finite pressure. The interest of this model is that it can be considered as a universal reference model for soft-core interactions in highly anisotropic molecules. Its dynamics is not as involved as the dynamics of hard-core models while having the same conceptual simplicity. Continuous potential models are transferable and can be made more complicated to simulate more realistic molecules. At present, however, realistic models are too heavy computationally to allow a systematic study of the phase diagram. The dynamics of even the simplest liquid–crystalline systems is very costly in terms of computer time, and very delicate from the point of view of generating reliable trajectories. Having verified the existence of mesophases, we will

proceed in a subsequent work to the study of their relative stability through a thermodynamical analysis of the model.

We thank D. Frenkel, M. L. Klein, I. R. McDonald, and L. F. Rull for interesting discussions. Most numerically intensive calculations were carried out on a IBM 3090-600E VF computer at IBM ECSEC in Rome. We also acknowledge a contribution from the Italian CNR via the Cray Project on Statistical Mechanics and the Progetto Finalizzato 'Sistemi Informatici e Calcolo Parallelo'.

References

[1] VERTOGEN, G. and DE JEU, W. H., 1988, *Thermotropic Liquid Crystals, Fundamentals* (Springer).
[2] DE GENNES, P. G., 1974, *The Physics of Liquid Crystals* (Oxford University Press).
[3] ZANNONI, C., 1979, *The Molecular Physics of Liquid Crystals*, edited by G. R. Luckhurst and G. W. Gray (Academic Press).
[4] GAY, J. G. and BERNE, B. J., 1981, *J. chem. Phys.*, **74**, 3316.
[5] BERNE, B. J. and PECHUKAS, P., 1972, *J. chem. Phys.*, **56**, 4213.
[6] ADAMS, D. J., LUCKHURST, G. R. and PHIPPEN, R. W., 1987, *Molec. Phys.*, **61**, 1575.
[7] DE MIGUEL, E., RULL, L. F., CHALAM, M. K., GUBBINS, K. E. and VAN SWOL, F., 1991, *Molec. Phys.*, **72**, 593.
[8] DE MIGUEL, E., RULL, L. F., CHALAM, M. K. and GUBBINS, K. E., 1991, *Molec. Phys.*, **74**, 405.
[9] CHALAM, M. K., GUBBINS, K. E., DE MIGUEL, E. and RULL, L. F., 1991, *Molec. Sim.*, **7**, 357.
[10] LUCKHURST, G. R., STEPHENS, R. A. and PHIPPEN, R. W., 1991, *Liq. Crystals*, **8**, 451.
[11] EGBERTS, E. and BERENDSEN, H. J. C., 1988, *J. chem. Phys.*, **89**, 3718.
[12] PICKEN, S. J., VAN GUNSTEREN, W. F., VAN DUIJNEN, P. TH. and DE JEU, 1989, *Liq. Crystals*, **6**, 357.
[13] ONO, I. and KONDO, S., 1991, *Molec. Crystals liq. Crystals Lett.*, **8**, 69.
[14] WILSON, M. R. and ALLEN, M. P., 1991, *Molec. Crystals liq. Crystals*, **198**, 465; WILSON, M. R. and ALLEN, M. P., 1992, *Liq. Crystals*, **12**, 157.
[15] EPPENGA, R. and FRENKEL, D., 1984, *Molec. Phys.*, **52**, 1303.
[16] FRENKEL, D., MULDER, B. M. and MACTAGUE, J. P., 1984, *Phys. Rev. Lett.*, **52**, 287.
[17] FRENKEL, D. and MULDER, B. M., 1985, *Molec. Phys.*, **55**, 1171.
[18] STROOBANTS, A., LEKKERKERKER, H. N. W. and FRENKEL, D., 1986, *Phys. Rev. Lett.*, **57**, 1452.
[19] VEERMAN, J. A. C. and FRENKEL, D., 1989, *Physica* A, **156**, 599.
[20] VEERMAN, J. A. C. and FRENKEL, D., 1990, *Phys. Rev.* A, **41**, 3237.
[21] VEERMAN, J. A. C. and FRENKEL, D., 1991, *Phys. Rev.* A, **43**, 4334.
[22] CICCOTTI, C. and RYCKAERT, J. P., 1986, *Comp. Phys. Rep.*, **4**, 345; CICCOTTI, C., FERRARIO, M. and RYCKAERT, J. P., 1982, *Molec. Phys.*, **47**, 1253.
[23] NOSÉ, S., 1984, *Molec. Phys.*, **52**, 255.
[24] PARRINELLO, M. and RAHMAN, A., 1980, *Phys. Rev. Lett.*, **45**, 1196.
[25] PARRINELLO, M. and RAHMAN, A., 1981, *J. Appl. Phys.*, **52**, 7182.
[26] NOSÉ, S. and KLEIN, M. J., 1983, *Molec. Phys.*, **50**, 1055.
[27] FERRARIO, M. and RYCKAERT, J. P., 1985, *Molec. Phys.*, **54**, 587.
[28] HANSEN, J. P. and MACDONALD, I. R., 1986, *Theory of Simple Liquids*, second edition (Academic Press).
[29] HESS, S., FRENKEL, D. and ALLEN, M. P., 1991, *Molec. Phys.*, **74**, 765.
[30] DE MIGUEL, E., RULL, L. F. and GUBBINS, K. E., 1992, *Phys. Rev.* A, **45**, 3813.